International Journal of Engineering Inventions
e-ISSN: 2278-7461, p-ISSN: 2319-6491
Volume 12, Issue 10 [October. 2023] PP: 102-115

A lifespan decline prediction method of proton exchange membrane fuel cell based on frequency enhanced decomposed transformer

Chunxiao Feng [*], Yan sun, Xing Shu, Wei Guo

School of Automotive Engineering, Shandong Jiaotong University, Jinan, 250037, China

[*] *Corresponding author: Chunxiao Feng (e-mail: feng_chunxiao99@163.com)*

Abstract:
Proton exchange membrane fuel cell (PEMFC) systems are emerging as one of the most promising carbon-neutral transportation alternatives. Durability continues to be the key barrier to its widespread commercialization, nevertheless. The development of timely optimization strategies that increase the durability of PEMFC is facilitated by the establishment of an accurate model to forecast the aging state of the device. To solve the problem of predicting the life decline of PEMFC, this paper proposes a lifespan decline prediction method of proton exchange membrane fuel cell based on frequency enhanced decomposed transformer (Fedformer). This article establishes an experimental platform and conducts life testing on the PEMFC test platform, obtaining a mixed dataset consisting of a national standard operating condition degradation dataset and a real vehicle operating condition degradation dataset. The dataset was preprocessed through wavelet threshold denoising. Establishing a Fedformer model, by adding a fourier enhancement module based on Transformer, the frequency domain features of the data can be extracted, the prediction accuracy can be improved, and the prediction results can be compared and evaluated. The prediction results demonstrate the accuracy and universality of the proposed Fedformer based PEMFC life decline prediction method.

Keywords: *Proton exchange membrane fuel cell; Lifespan decline prediction; Frequency enhanced decomposed transformer*

Date of Submission: 05-10-2023 Date of acceptance: 19-10-2023

I. Introduction

Due to the international economy's rapid growth, human consumption of energy is also increasing. Traditional fossil energy has been unable to meet human needs, and new energy is needed to replace traditional fossil energy [1–3]. Among them, fuel cells have become promising energy conversion equipment by converting electric energy through electrochemical reactions [4]. PEMFC is the mainstream product of fuel cells. In order to ensure its long-term and economic feasibility, it is very important to estimate the health status of PEMFC, and the most critical problem is to accurately predict its decline. This is also an important basis for the healthy prognosis of PEMFC [5, 6]. Nowadays, scholars at home and abroad have proposed various prediction methods to estimate the declining state of PEMFC. These strategies can generally be divided into two categories: model-based and data-driven [7, 8].

The model-based method generally and intuitively reveals the physical mechanism of internal degradation of fuel cells by establishing a series of mathematical equations, which can be divided into the establishment of an empirical model, a semi-empirical model, or a physical model of PEMFC, and the prediction of degradation can be realized through statistics, filtering, machine learning, and other methods [9–11]. Jouin et al. [12] proposed a voltage life degradation model considering all parameters of fuel cells and used different mathematical models based on time to describe the degradation rate of parameter variables. Hu et al. [13] proposed a fuel cell reconfiguration model for a hybrid electric city bus to predict its life. From the viewpoints of thermodynamics and economics, Chen et al. [14] established a new degradation model and investigated the changes in instantaneous voltage, degradation rate, electric power, and efficiency under various working currents and their effects on the life-cycle cost of battery packs. Mao et al. [15] proposed a method to predict the performance change of PEMFC by predicting the parameters of aging model. It is very challenging to develop a high-precision physical decay model because the decay solution of a fuel cell is a complicated multi-physical field coupling problem and is unobservable in many respects [16]. Some scholars call model-based and data-driven methods hybrid methods, which combine the advantages of model-based and data-driven methods [17]. Zhou et al. [18] used the sliding window method to combine the nonlinear autoregressive neural network with the

voltage degradation model to realize the three steps of training verification prediction in each sliding window. Cheng et al. [19] proposed a residual service life prediction method based on least squares support vector machines and regularized particle filters. However, in most cases, the coupling of the two methods needs to establish a model with higher rationality, and the hybrid method still needs to understand the degradation mechanism of PEMFC in advance [20, 21]. Therefore, model-based, and data-driven hybrid methods are also classified as model-based prediction methods by most scholars.

Different from the model-based method, the data-driven method can be regarded as a "black box" to build a high-order nonlinear relationship between input and output signals. The future decline state is based on the historical decline trend, and it is no longer necessary to use an accurate mathematical or analytical model to reveal the detailed degradation mechanism of PEMFC [22–24]. Data-driven strategies mainly study artificial intelligence models such as adaptive neurofuzzy inference system [25], echo state network [26], correlation vector machine [27], support vector machine [28], and Gaussian process state space mode [29]. Deep learning-based PEMFC prediction has drawn greater interest recently, such as in artificial neural networks [30] and long-term and short-term memory neural networks [31, 32]. Zuo et al. [33] compared the short-term voltage prediction effects of four deep learning methods: LSTM, gating cycle unit, attention-based LSTM, and attention-based Gru. Ma et al. [34] propose a fuel cell performance data fusion prediction method based on LSTM and ARIMA. Wang et al. [35] propose to use stacked LSTM to predict the short-term aging trend of fuel cells under dynamic conditions. stacked LSTM uses the differential evolution algorithm to optimize various parameters in LSTM. Ma et al. [36] proposed a Grid LSTM model to predict the aging trend of fuel cells under constant conditions and verified the model with 1 kW, 1.2 kW, and 25 kW fuel cells, respectively.

One of the research areas of PEMFC life decline is the investigation of more accurate forecast techniques. Additionally, the procedures' efficacy and accuracy need to be increased. The Fedformer introduced in this paper is based on the transformer model, which adds the Fourier enhancement module. To increase the model's prediction accuracy, it uses frequency domain data after the Fourier transform for feature extraction rather than applying the transformer to the time feature extraction. At present, most of the aging prediction studies are carried out in a centralized way based on the data obtained under the same working conditions, without considering the universality of the prediction model. The aging life test of PEMFC before leaving the factory does not necessarily use the real vehicle's working conditions, or it will be different from the driver's habits. Therefore, the training data may not be generated under the same working conditions. Therefore, this paper uses the aging data of national standard working conditions as the training data. In order to assess the model universality of LSTM and Fedformer, aging data from actual car operating situations are used as training data. The following are the primary innovations in this paper:

1) In contrast to LSTM and other models, which focus on data features from a time domain perspective, Fourier enhancement module of Fedformer can extract features from a frequency domain perspective, preprocess the data set with wavelet threshold de-noising, decompose and filter noise and unknown interference, and de-noise the input data set. These features all work to increase the predictive accuracy of the model.

2)The data set in this paper combines the aging parameters of the same test bench under two different working conditions. It is demonstrated that the model trained by Fedformer has strong universality by using the parameters of national standard working circumstances to estimate the aging trend of PEMFC under real car working settings.

The remainder of this essay is structured as follows: The experimental data set is preprocessed and experimental settings are established in Section 2 in order to gather data for the life test. Section 3 introduces the framework structure and discusses the predicted results. The conclusion can be found in Section 4.

II. PEMFC life test and data set preprocessing

The 90kw PEMFC test bench used in this experiment is shown in Fig. 1, which is mainly composed of four parts: an air supply device, a cooling circulation device, an electronic load, and a data acquisition device. Fig. 1 (a) is the structural diagram of a simplified test bench; Fig. 1 (b) is the physical diagram of the test bench, which can be utilized for testing PEMFC's long-term dynamic durability and polarization. The following is a brief introduction to each part: ①gas supply device: during the operation of the PEMFC stack, the gas supply device needs to provide reaction gas continuously. In this experiment, the gas supply device is divided into a hydrogen supply device and an air supply device. The hydrogen is produced by the hydrogen storage tank and supplied by the hydrogen storage tank after the air has been compressed, filtered, and stored in the gas storage tank. ② Keeping the PEMFC stack within the required temperature range is necessary for normal operation of the cooling circulation system, usually 30 °C–80 °C. When the temperature of the stack is low at the beginning of operation, the water tank will automatically raise the temperature, and the heated deionized water will flow into the stack through the water pump to raise the temperature. When the stack temperature is too high, the circulating water flows through the cooling pipe and the water pump to cool it down. ③Electronic load: it is vital to employ an external electronic load who's current, voltage, and power range must be higher than the stack itself in order to

satisfy the experimental design and imitate the real load conditions to test the performance and deterioration of the PEMFC. ④Data acquisition device: in order to keep track of the stack's current condition immediately, the test bench is required to be able to collect PEMFC data in real time. After the bench is started, it will automatically collect data; all collected data will be stored in the background, and important information will be displayed on the main control interface in real time. The main data collected by the system include stack voltage, current, power, gas temperature, pressure, circulating water temperature and flow, and many other variables.

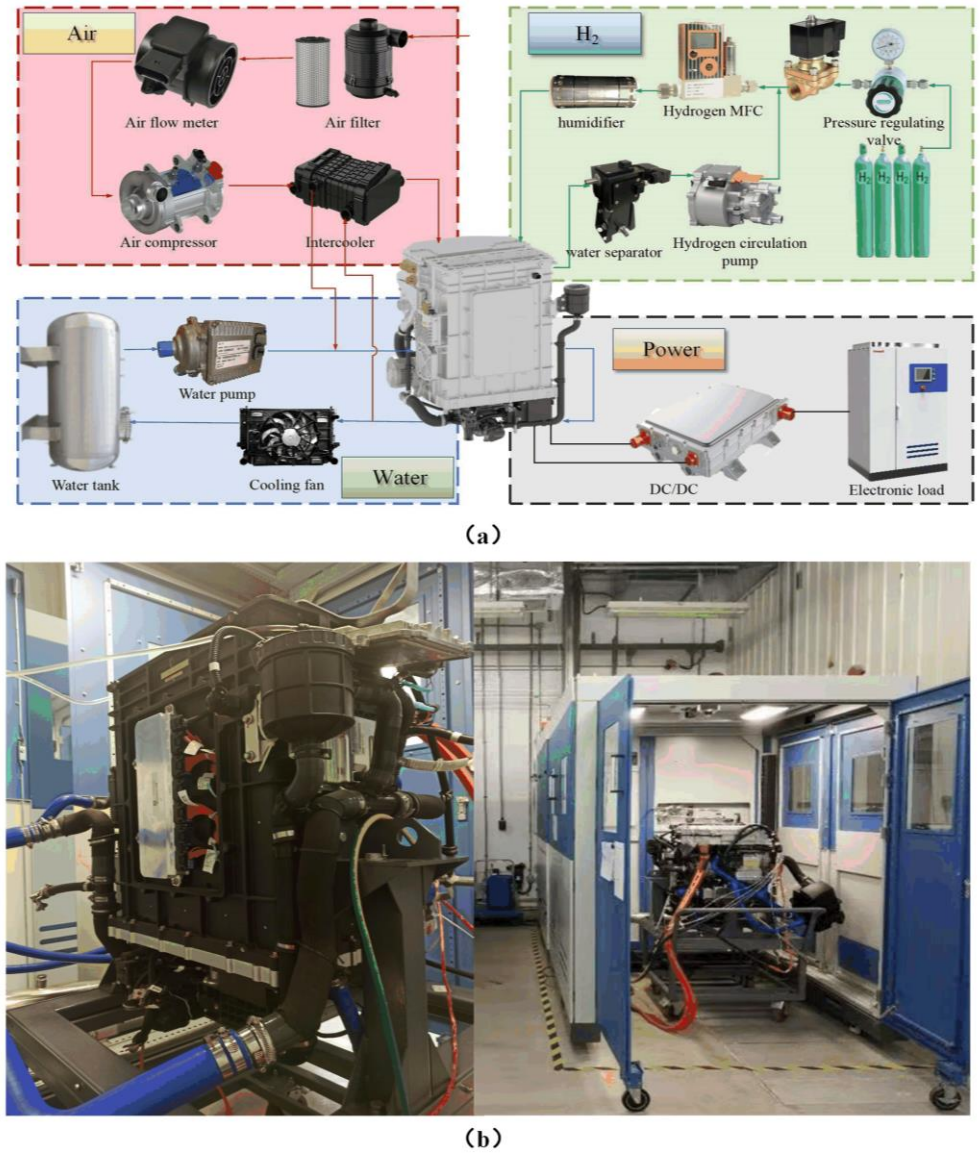

Fig. 1. PEMFC System (a) Schematic diagram of PEMFC system composition (b) PEMFC Test Bench

The working conditions used in the experiment are shown in Fig. 2. The experiment is split into two sections. The first part of the 2000h durability experiment uses the GB/T 38914-2020 vehicle proton exchange membrane PEMFC stack service life test evaluation method, and the second part of the 500h durability experiment uses the CLTC-P China passenger vehicle driving cycle for testing. The GB/T 38914-2020 evaluation technique for the service life of PEMFC stacks for cars includes idle, start-stop, rated, and variable load conditions. In the experiment, the test is carried out in the order of these four conditions. Each condition has an operation cycle of 4 hours, and after every 4 hours of operation, shut down and rest for 1 hour. The driving cycle length of the CLTC-P Chinese passenger car is 1800km. By disrupting and reorganizing the driving cycle, it is combined into 1000 driving cycles, forming a 500-hour driving cycle for the CLTC-P Chinese passenger car. The working condition composition diagram of the article is shown in Fig. 2.

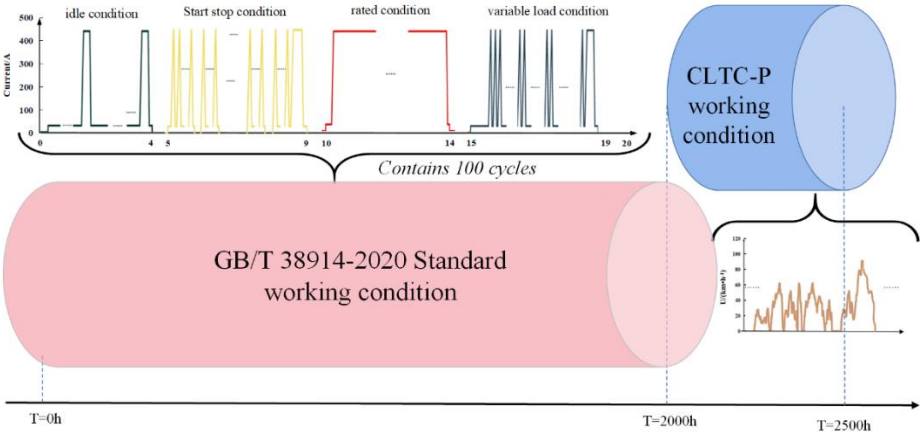

Fig. 2. Composition of Working Conditions

Input 2000h of national standard working conditions and 500h of CLTC-P working conditions into the test bench for the life test and obtain data. Parameters in the data set include stack voltage, current, cathode temperature, anode temperature, cathode pressure, anode pressure, cathode flow, anode flow, the inlet and outlet temperature of cooling water, the flow of cooling water, and other variables of the PEMFC stack. This experiment draws and describes the attenuation trend and polarization curve of the output voltage. The polarization curve of the experimental results is shown in Fig. 3. When the control current density is 0.9 A/cm2 and the time nodes are 0h, 500h, 1000h, 1500h, 2000h, and 2500h, respectively, the stack voltage is 246V, 239V, 233V, 227V, 222V, and 220V, respectively. It is discovered that when stack operation time increases, stack voltage falls.

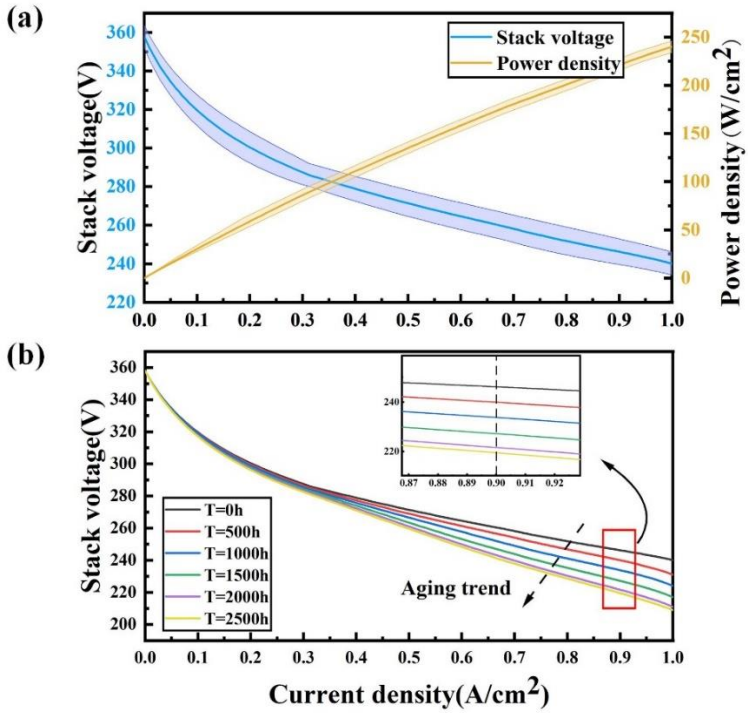

Fig. 3. Polarization Curve (a) Variation of Stack Voltage and Power Density
(b) polarization curve with time

Next, the data set is preprocessed. Since the first 2000h of the data set is the accelerated life test data obtained according to the national standard operating conditions and the machine is frequently switched on and off, the data waveform has more ups and downs, so it is necessary to use wavelet threshold denoising to denoise the data set, which can make the subsequent neural network have a better training effect. The main idea is to use the characteristic that the amplitude of the wavelet coefficients of the signal is greater than that of the noise after multi-scale wavelet decomposition of the noisy signal to extract the wavelet coefficients of the original signal.

Create an artificial threshold, preserve all wavelet coefficients above the threshold, and set the wavelet coefficients whose amplitude is below the threshold to 0.

Using the wavelet denoising toolbox of MATLAB, set the parameter wavelet base to db5, the decomposition level to 8, the denoising method to minimax, the threshold rule to soft threshold, and the threshold of each level to the default value. For the operation data denoising of the PEMFC stack, the waveform comparison of the PEMFC stack voltage before and after denoising is shown in Fig. 4. The figure shows how the wavelet threshold denoising algorithm can successfully remove the noise in the original data while keeping the stack's decay information. The comparison curve of PEMFC average single cell voltage and internal resistance decay before and after denoising is shown in Fig. 4.

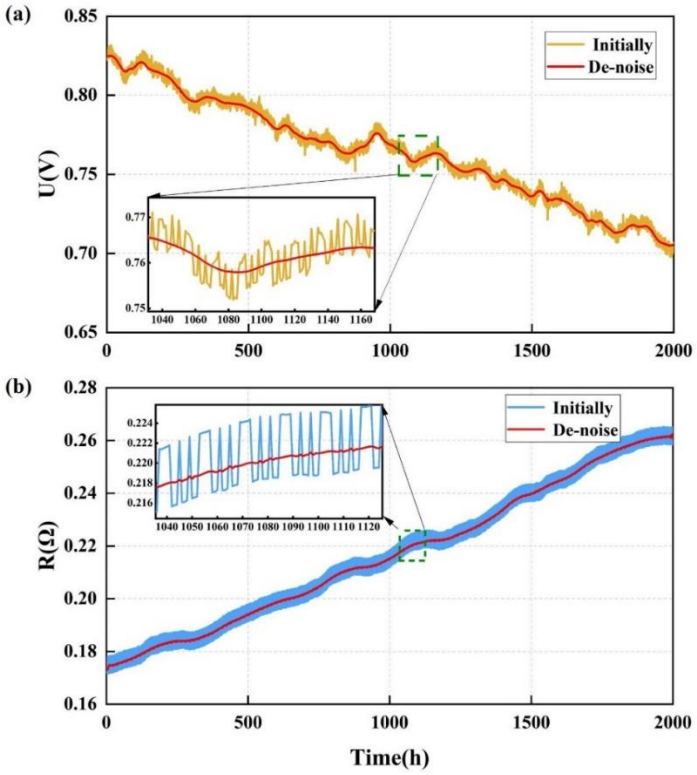

Fig. 4. Waveform comparison before and after denoising(a) Average single cell voltage (b) Internal resistance

III. Modeling and forecasting based on Fedformer

3.1 Fedformer model building

Fedformer is based on the Transformer model. While inheriting the parallel computing ability of Transformer, it can extract the frequency domain characteristics of data and enhance the prediction accuracy by adding a Fourier enhancement module based on Transformer. The structure of Fedformer is composed of n encoders and m decoders, as shown in Figure 5, which is the structural schematic diagram of Fedformer.

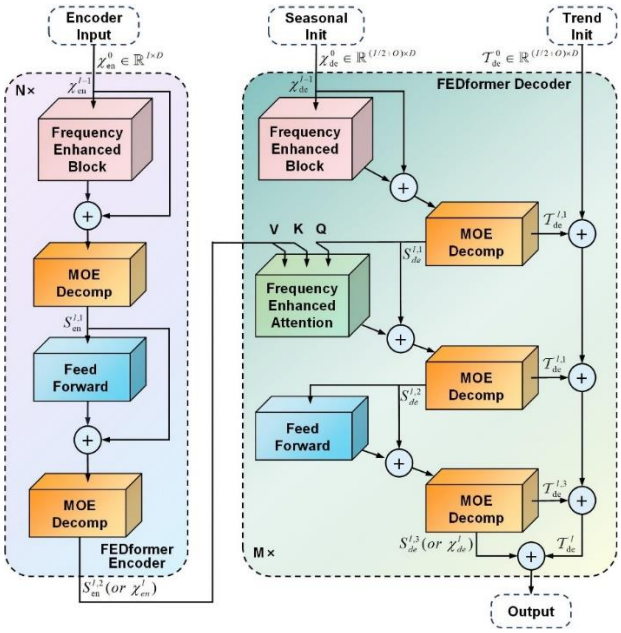

Fig. 5. Schematic Diagram of the Fedformer Structure

The encoder in Fig. 5 adopts a multi-layer structure as follows:

$$\begin{aligned} S_{en}^{l,1}, \_ &= MOEDecomp(FEB(X_{en}^{l-1}) + X_{en}^{l-1}), \\ S_{en}^{l,2}, \_ &= MOEDecomp(FeedForward(S_{en}^{l,1}) + S_{en}^{l,1}), \\ X_{en}^{l} &= S_{en}^{l,2}, \end{aligned} \tag{1}$$

Where $S_{en}^{l,1}$, i∈{1, 2} represents the seasonal component after the i-th decomposition block of the first layer.

The decoder in Fig. 5 also adopts a multi-layer structure, as follows:

$$\begin{aligned} S_{de}^{l,1}, T_{de}^{l,1} &= MOEDecomp(FEB(X_{de}^{l-1}) + X_{\mathrm{de}}^{l-1}), \\ S_{de}^{l,2}, T_{de}^{l,2} &= MOEDecomp(FEA(S_{de}^{l,1}, X_{en}^{N}) + S_{\mathrm{de}}^{l,1}), \\ S_{de}^{l,3}, T_{de}^{l,3} &= MOEDecomp(FeedForward(S_{de}^{l,2}) + S_{\mathrm{de}}^{l,2}), \\ X_{de}^{l} &= S_{de}^{l,3}, \\ T_{de}^{l} &= T_{de}^{l-1} + W_{l,1} \cdot T_{de}^{l,1} + W_{l,2} \cdot T_{de}^{l,2} + W_{l,3} \cdot T_{de}^{l,3}, \end{aligned} \tag{2}$$

Where $S_{de}^{l,i}$, $T_{de}^{l,i}$, i∈{1, 2, 3} respectively, represent the seasonal component and trend component after the i-th decomposition block of the first layer. $W_{l,i}$. i∈{1, 2, 3} represents the trend $T_{de}^{l,i}$ extracted for the i-th time.

In Fedformer, one of the most important problems is which frequency division quantum set is used for Fourier analysis. Retaining low-frequency and discarding high-frequency components is a typical approach, but this may not be appropriate for time series prediction because some trend changes in time series are connected to significant events. This portion of the information can be lost if all high-frequency components are simply deleted. According to the theoretical analysis of Zhou et al. [38], the random selection of frequency division quantum sets, including low-frequency components and high-frequency components, can better represent the time series.

The data set used in this paper is divided into two parts: the first 2000h data set is obtained from the life test experiment required by the national standard, and the last 500h data set is the aging data set, which, in order to replicate the operation of the actual vehicle, was put together in accordance with the CLTC-P working conditions. Use the aging data of the first 2000h under the national standard working condition for model training, and then use the aging data of the last 500h under the real vehicle working condition for prediction. This is to better simulate the aging test of PEMFC using national standard conditions before leaving the factory, and the actual operation is closer to the characteristics of real vehicle conditions. The overall structure of the article is shown in Fig. 6.

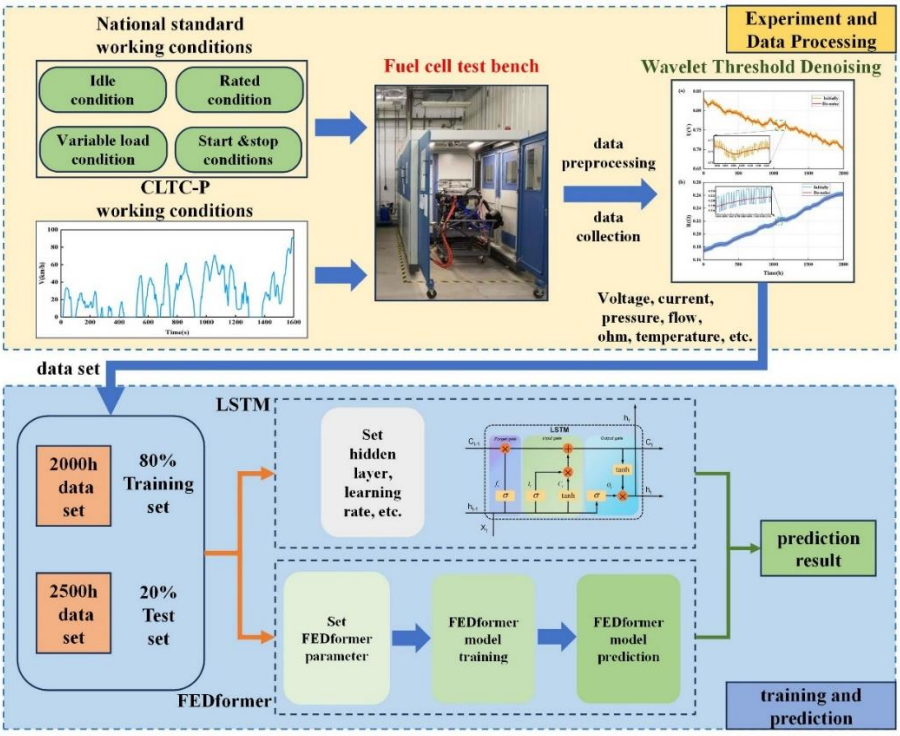

Fig.6. overall structure of the article

The LSTM configuration employed in this study has the following parameters: a hidden layer with 128 neurons; a loss function of average absolute error; an optimizer named Adam; an epichs of 100; a batch size of 20; and a learning efficiency of 0.005. The Fedformer neural network code used in this paper is public data, and refers to the code used in Zhou et al. [38]. Because the use of national standard working conditions as the training set and the actual working conditions as the prediction data may significantly affects the outcome of the prediction, this paper not only predicts the complete data set under 2500h but also predicts the national standard working conditions under 2000h in advance and compares neural network prediction results under the two data sets. For a separate 2000hour national standard working condition data set, 80% of the data is selected as training data, and 20% of the data is selected as prediction data.

3.2Comparison and discussion of prediction results

In this paper, the machine learning prediction model's prediction ability is assessed using the root mean square error (RMSE) and mean absolute percentage error (MAPE). The greater the model's ability to forecast outcomes is, the closer the values of RMSE and MAPE are to 0. The two indicators' calculating formula is as follows:

$$RMSE = \sqrt{\frac{1}{n}\sum_{t=1}^{n}\left(\hat{y}_i - y_i\right)^2} \tag{3}$$

$$MAPE = \frac{1}{n}\sum_{t=1}^{n}\frac{\left|\hat{y}_i - y_i\right|}{y_i} \tag{4}$$

Where $\hat{y}_i$ is the model output value and y_i is the measured value of the aging voltage.

Fig. 7(a) shows the LSTM model's forecasting outcomes trained with the previous 1600h data on the test data, and Fig. 7(b) shows the Fedformer model's forecasting outcomes trained with the previous 1600h data on the test data. The forecasting outcomes for the next 400 hours were verified and contrasted with the actual results. As illustrated in Fig. 7, the LSTM model's maximum prediction error is 0.0112V, and the Fedformer model's maximum prediction error is 0.0008V. Compared with the LSTM model, the developed Fedformer model has better prediction performance under the 2000h voltage decay data set.

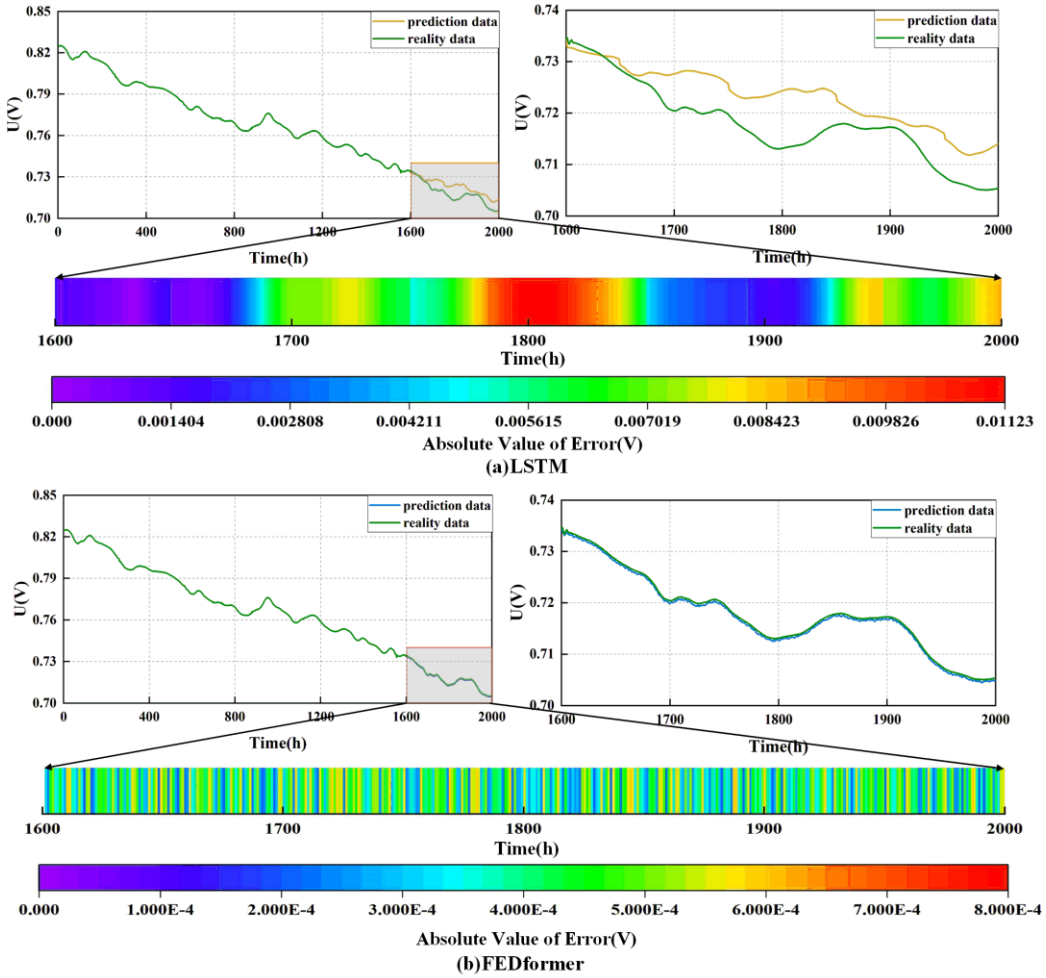

Fig. 7. 2000h voltage data set (a) LSTM prediction results (b) Fedformer prediction results

Fig.8(a) shows the LSTM model's forecasting outcomes trained with the data of the previous 2000h on the test data, and Fig.8(b) shows the Fedformer model's forecasting outcomes trained with the data of the previous 2000h on the test data. The forecasting outcomes for the next 500 hours were verified and contrasted with the actual results. As illustrated in Fig. 8, the LSTM model's maximum prediction error is 0.01V, and the Fedformer model's maximum prediction error is 0.0012V. Compared with the LSTM model, the developed Fedformer model has better prediction performance in the 2500h voltage decay data set.

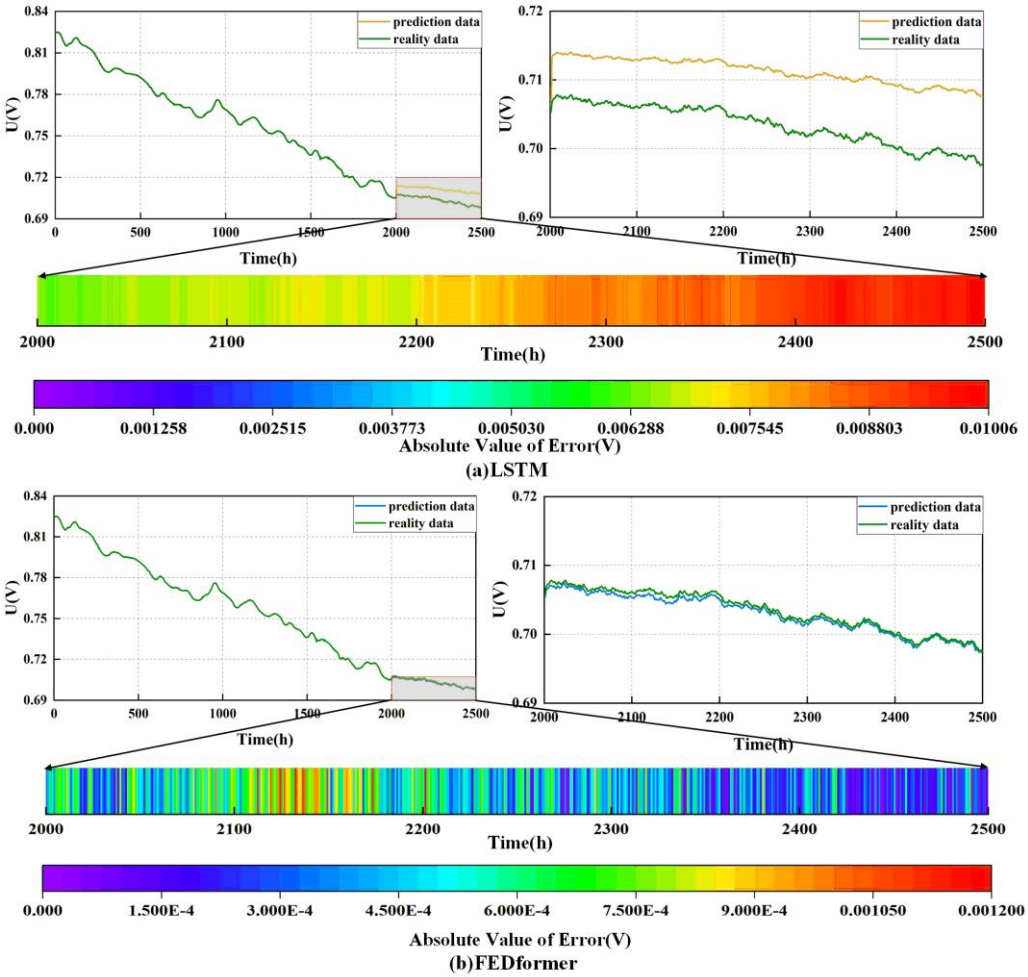

Fig. 8. 2500h voltage data set (a) LSTM prediction results (b) Fedformer prediction results

Fig. 9(a) shows the LSTM model's forecasting outcomes trained with the previous 1600h data on the test data, and Fig. 9(b) shows the Fedformer model's forecasting outcomes trained with the previous 1600h data on the test data. The forecasting outcomes for the next 400 hours were verified and contrasted with the actual results. As illustrated in Fig. 9, the LSTM model's maximum prediction error is 0.0021Ω, and the Fedformer model's maximum prediction error is 0.0007Ω. Compared with the LSTM model, the developed Fedformer model has better prediction performance under the 2000h reactor internal resistance decay data set.

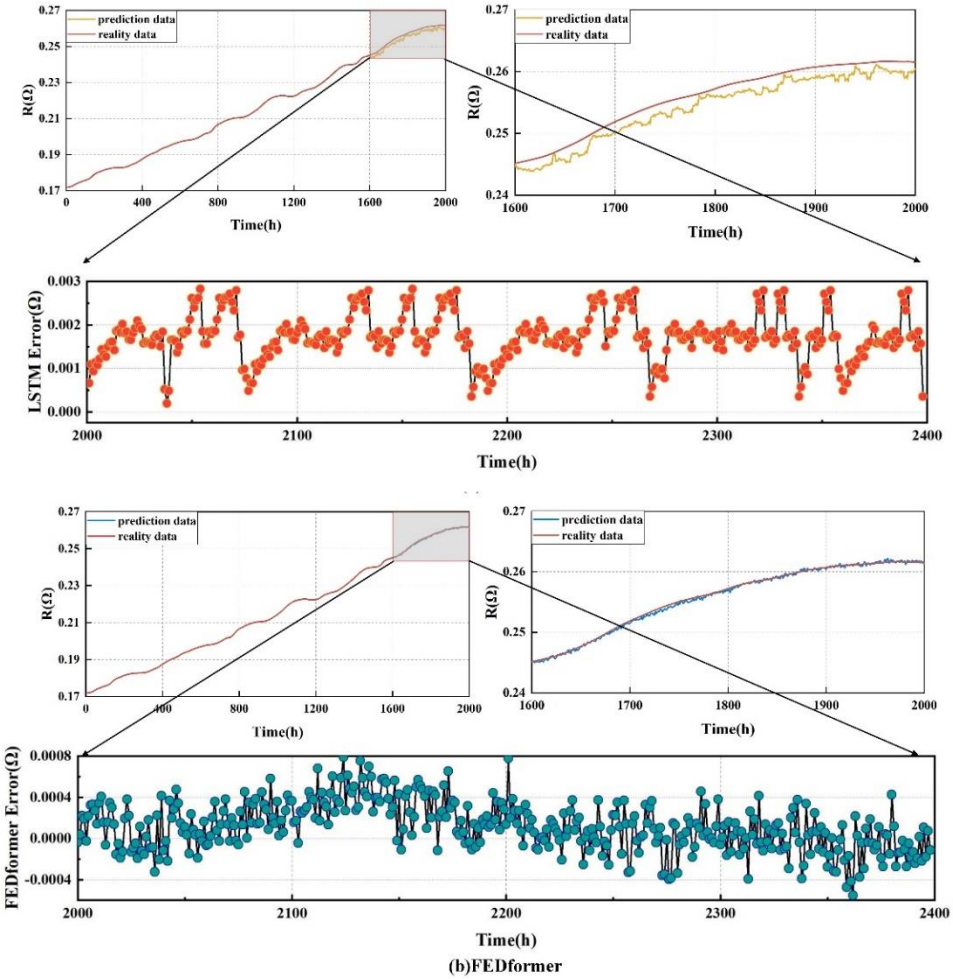

Fig. 9. 2000h internal resistance data set (a) LSTM prediction results (b) Fedformer prediction results

Fig. 10(a) shows the LSTM model's forecasting outcomes trained with the previous 2000h data on the test data, and Fig. 10(b) shows the Fedformer model's forecasting outcomes trained with the the previous 2000h data on the test data. The forecasting outcomes for the next 500 hours were verified and contrasted with the actual results. As illustrated in Fig. 10, the LSTM model's maximum prediction error is 0.0039Ω, and the Fedformer model's maximum prediction error is 0.0007Ω. Compared with the LSTM model, the developed Fedformer model has better prediction performance under the 2500h stack internal resistance decay data set.

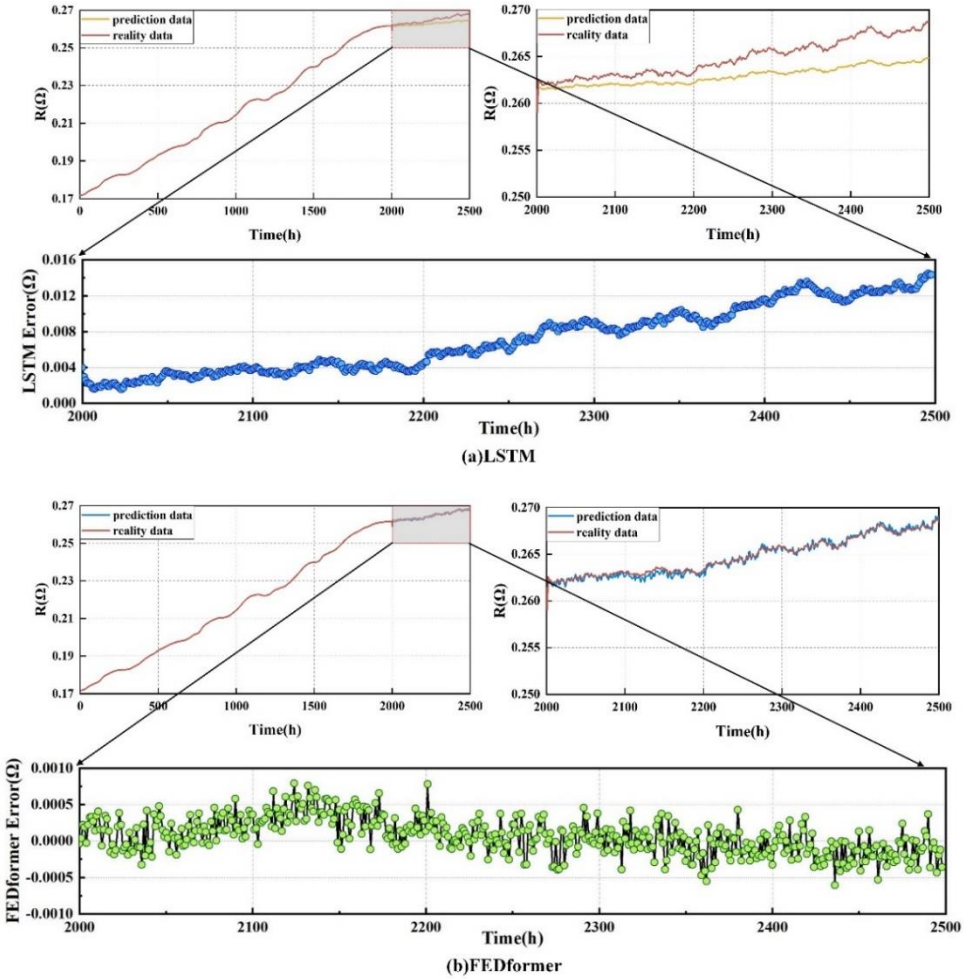

Fig. 10. 2500h internal resistance dataset (a) LSTM prediction results (b) Fedformer prediction results

This research employs root means square error and average absolute error as evaluation criteria to describe the prediction performance of LSTM more intuitively and Fedformer under varied data sets. The average absolute error of voltage is shown in Fig. 11(a). Under the 2000h data set and the 2500h data set, the average absolute error of the Fedformer is much less than that of the LSTM. The voltage's root mean square error is shown in Fig. 11(b). Like the average absolute error of voltage, the root mean square error of the Fedformer is less than LSTM. When LSTM predicts the 2000h data set and the 2500h data set, the root mean square error and average absolute error of the 2500h data set are greater than those of the 2000h data set. The reason is that the data of the last 500 h in the 2500h are obtained from the real vehicle conditions, which are different from the data of the previous 2000h national standard conditions. In contrast, for different data sets, the root means square error and mean absolute error of the prediction results of Fedformer are almost the same. In conclusion, it can be proved that Fedformer has better prediction accuracy and model universality than LSTM.

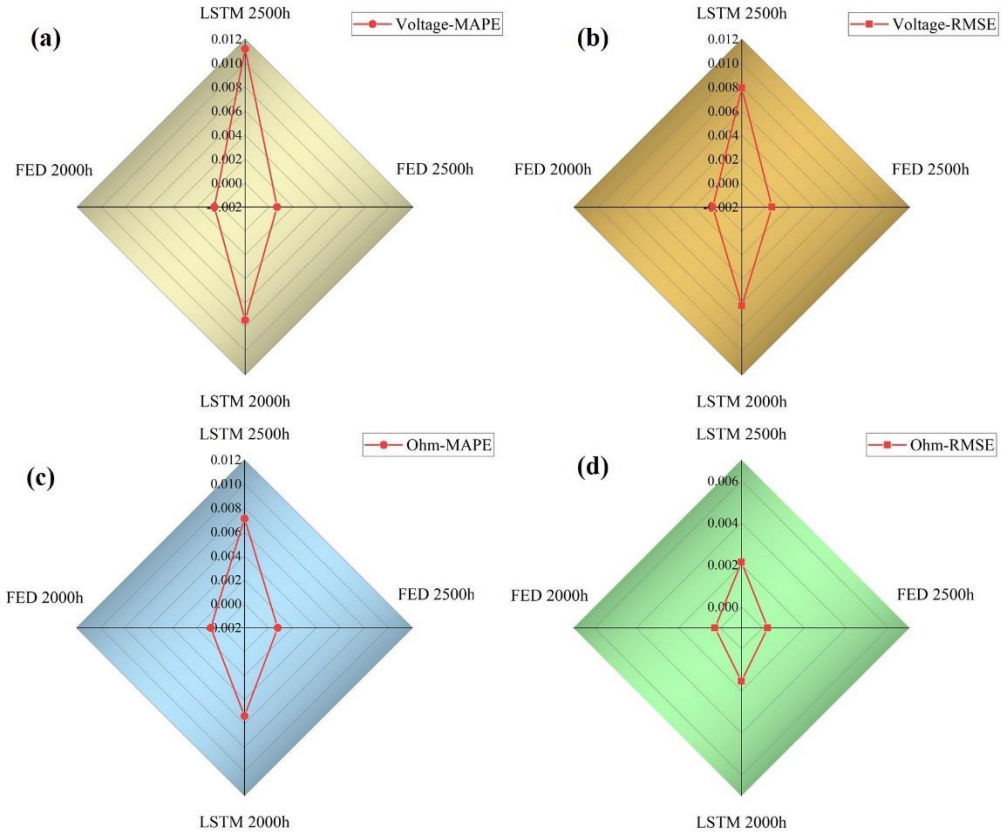

Fig. 11 comparison between root mean square error and mean absolute error

IV. Conclusion

The collected degradation time series data set is integrated with a machine learning method in this paper to forecast the voltage degradation and internal resistance deterioration of automobile PEMFC. The established prediction model has been verified and successfully used in short-term voltage attenuation prediction and short-term internal resistance attenuation prediction. The main research results of this paper are as follows:

(1) The PEMFC life-aging experiment was designed. The experimental national standard condition and the real vehicle condition were established, respectively. The national standard condition and real vehicle condition were input into the experimental bench, and the 2000-hour national standard condition aging data set and the 500-hour real vehicle condition aging data set were obtained.

(2) By comparing the prediction results of LSTM and Fedformer under the same data set, the MAPE and RMSE of Fedformer voltage under the 2500h data set are 0.0006 and 0.0005, the LSTM are 0.011 and 0.008, it is found that the prediction error of Fedformer is much smaller than that of LSTM, which demonstrates that the Fedformer prediction model outperforms the LSTM.

(3) By taking the 2000hour national standard condition aging data set as the training data, the life aging trend of PEMFC under 500hour real vehicle conditions is predicted. The MAPE and RMSE of the Fedformer voltage under 2500h are 0.0006 and 0.0005, under 2000h are 0.0005 and 0.0004. It is found that the prediction errors of Fedformer under different data sets are almost the same, which proves that the Fedformer prediction model is universal.

Conflicts of Interests

The authors declare that there is no conflict of interests regarding the publication of this paper.

Acknowledgments

The authors greatly appreciate the support from Shandong Jiaotong University Postgraduate Science and Technology Innovation Project with No.2023YK003, No.2023YK007.

References

[1]. Yin C, Gao Y, Li K, et al. Design and numerical analysis of air-cooled proton exchange membrane fuel cell stack for performance optimization[J]. Energy Conversion and Management, 2021, 245: 114604.

[2]. Wan Y, Qiu D, Yi P, et al. Design and optimization of gradient wettability pore structure of adaptive PEM fuel cell cathode catalyst layer[J]. Applied Energy, 2022, 312: 118723.

[3]. Wang G, Yu Y, Liu H, et al. Progress on design and development of polymer electrolyte membrane fuel cell systems for vehicle applications: A review[J]. Fuel Processing Technology, 2018, 179: 203-228.

[4]. Jouin M, Bressel M, Morando S, et al. Estimating the end-of-life of PEM fuel cells: Guidelines and metrics[J]. Applied energy, 2016, 177: 87-97.

[5]. Muhsen D H, Ghazali A B, Khatib T. Multiobjective differential evolution algorithm-based sizing of a standalone photovoltaic water pumping system[J]. Energy Conversion and Management, 2016, 118: 32-43.

[6]. Hu Z, Xu L, Li J, et al. A reconstructed fuel cell life-prediction model for a fuel cell hybrid city bus[J]. Energy conversion and management, 2018, 156: 723-732.

[7]. Zhang X, Yang D, Luo M, et al. Load profile based empirical model for the lifetime prediction of an automotive PEM fuel cell[J]. International Journal of Hydrogen Energy, 2017, 42(16): 11868-11878.

[8]. Lechartier E, Laffly E, Péra M C, et al. Proton exchange membrane fuel cell behavioral model suitable for prognostics[J]. International Journal of Hydrogen Energy, 2015, 40(26): 8384-8397.

[9]. Jouin M, Gouriveau R, Hissel D, et al. Degradations analysis and aging modeling for health assessment and prognostics of PEMFC[J]. Reliability Engineering & System Safety, 2016, 148: 78-95.

[10]. Hu Z, Xu L, Li J, et al. A reconstructed fuel cell life-prediction model for a fuel cell hybrid city bus[J]. Energy conversion and management, 2018, 156: 723-732.

[11]. Zhang D, Baraldi P, Cadet C, et al. An ensemble of models for integrating dependent sources of information for the prognosis of the remaining useful life of Proton Exchange Membrane Fuel Cells[J]. Mechanical Systems and Signal Processing, 2019, 124: 479-501.

[12]. Chen X, Xu J, Yang C, et al. Thermodynamic and economic study of PEMFC stack considering degradation characteristic[J]. Energy Conversion and Management, 2021, 235: 114016.

[13]. Lechartier E, Laffly E, Péra M C, et al. Proton exchange membrane fuel cell behavioral model suitable for prognostics[J]. International Journal of Hydrogen Energy, 2015, 40(26): 8384-8397.

[14]. Mao L, Jackson L, Jackson T. Investigation of polymer electrolyte membrane fuel cell internal behaviour during long term operation and its use in prognostics[J]. Journal of Power Sources, 2017, 362: 39-49.

[15]. Ding C, Xu J, Xu L. ISHM-based intelligent fusion prognostics for space avionics[J]. Aerospace Science and Technology, 2013, 29(1): 200-205.

[16]. Zhang X, Pisu P. An Unscented Kalman Filter Based Approach for the Health Monitoring and Prognostics of a Polymer Electrolyte Membrane Fuel Cell[C]//Annual Conference of the PHM Society. 2012, 4(1).

[17]. Jouin M, Gouriveau R, Hissel D, et al. Prognostics of PEM fuel cell in a particle filtering framework[J]. International Journal of Hydrogen Energy, 2014, 39(1): 481-494.

[18]. Zhou D, Gao F, Breaz E, et al. Degradation prediction of PEM fuel cell using a moving window based hybrid prognostic approach[J]. Energy, 2017, 138: 1175-1186.

[19]. Cheng Y, Zerhouni N, Lu C. A hybrid remaining useful life prognostic method for proton exchange membrane fuel cell[J]. International Journal of Hydrogen Energy, 2018, 43(27): 12314-12327.

[20]. Ramasso E, Gouriveau R. Remaining useful life estimation by classification of predictions based on a neuro-fuzzy system and theory of belief functions[J]. IEEE Transactions on Reliability, 2014, 63(2): 555-566.

[21]. Mezzi R, Morando S, Steiner N Y, et al. Multi-reservoir echo state network for proton exchange membrane fuel cell remaining useful life prediction[C]//IECON 2018-44th annual conference of the IEEE industrial electronics society. IEEE, 2018: 1872-1877.

[22]. Xiong R, Sun F, Gong X, et al. A data-driven based adaptive state of charge estimator of lithium-ion polymer battery used in electric vehicles[J]. Applied Energy, 2014, 113: 1421-1433.

[23]. Liu H, Liu Z, Jia W, et al. Remaining useful life prediction using a novel feature-attention-based end-to-end approach[J]. IEEE Transactions on Industrial Informatics, 2020, 17(2): 1197-1207.

[24]. He K, Liu Z, Sun Y, et al. Degradation prediction of proton exchange membrane fuel cell using auto-encoder based health indicator and long short-term memory network[J]. International Journal of Hydrogen Energy, 2022, 47(82): 35055-35067.

[25]. Mao L, Jackson L. Selection of optimal sensors for predicting performance of polymer electrolyte membrane fuel cell[J]. Journal of Power Sources, 2016, 328: 151-160.

[26]. Morando S, Jemei S, Hissel D, et al. Proton exchange membrane fuel cell ageing forecasting algorithm based on Echo State Network[J]. International Journal of Hydrogen Energy, 2017, 42(2): 1472-1480.

[27]. Wu Y, Breaz E, Gao F, et al. Nonlinear performance degradation prediction of proton exchange membrane fuel cells using relevance vector machine[J]. IEEE Transactions on Energy Conversion, 2016, 31(4): 1570-1582.

[28]. Han I S, Chung C B. Performance prediction and analysis of a PEM fuel cell operating on pure oxygen using data-driven models: A comparison of artificial neural network and support vector machine[J]. International Journal of Hydrogen Energy, 2016, 41(24): 10202-10211.

[29]. Wang T, Zhou H, Zhu C. A short-term and long-term prognostic method for PEM fuel cells based on Gaussian process regression[J]. Energies, 2022, 15(13): 4844.

[30]. Tian P, Liu X, Luo K, et al. Deep learning from three-dimensional multiphysics simulation in operational optimization and control of polymer electrolyte membrane fuel cell for maximum power[J]. Applied Energy, 2021, 288: 116632.

[31]. Wu Y, Yuan M, Dong S,et al.Remaining useful life estimation of engineered systems using vanilla LSTM neural networks[J].NEUROCOMPUTING, 2018:S0925231217309505.

[32]. Liu J, Li Q, Chen W, et al. Remaining useful life prediction of PEMFC based on long short-term memory recurrent neural networks[J]. International Journal of Hydrogen Energy, 2019, 44(11): 5470-5480.

[33]. Zuo J, Lv H, Zhou D, et al. Deep learning based prognostic framework towards proton exchange membrane fuel cell for automotive application[J]. Applied Energy, 2021, 281: 115937.

[34]. Ma R, Li Z, Breaz E, et al. Data-fusion prognostics of proton exchange membrane fuel cell degradation[J]. IEEE Transactions on Industry Applications, 2019, 55(4): 4321-4331.

[35]. Ma R, Yang T, Breaz E, et al. Data-driven proton exchange membrane fuel cell degradation predication through deep learning method[J]. Applied energy, 2018, 231: 102-115.

[36]. Wang F K, Cheng X B, Hsiao K C. Stacked long short-term memory model for proton exchange membrane fuel cell systems degradation[J]. Journal of Power Sources, 2020, 448: 227591.

[37]. Wang F K, Mamo T, Cheng X B. Bi-directional long short-term memory recurrent neural network with attention for stack voltage degradation from proton exchange membrane fuel cells[J]. Journal of Power Sources, 2020, 461: 228170.
[38]. Zhou T, Ma Z, Wen Q, et al. Fedformer: Frequency enhanced decomposed transformer for long-term series forecasting[C]//International Conference on Machine Learning. PMLR, 2022: 27268-27286.